Inorg. Chem. **2006**, *45*, 4592–4601

Boxes, Helicates, and Coordination Polymers: A Structural and Magnetochemical Investigation of the Diverse Coordination Chemistry of Simple Pyridine-Alcohol Ligands

Shane G. Telfer,*[,†,#] Reiko Kuroda,[†,‡] Julie Lefebvre,[§] and Daniel B. Leznoff[§]

JST ERATO Kuroda Chiromorphology Project, Park Building, 4-7-6 Komaba, Meguro-ku, Tokyo, 153-0041 Japan, Graduate School of Arts and Sciences, University of Tokyo, Komaba, Meguro-ku, Tokyo, 153-8902 Japan, and Department of Chemistry, Simon Fraser University, 8888 University Drive, Burnaby, British Columbia, Canada V5A 1S6

Received October 5, 2005

A structurally diverse array of polynuclear complexes has been identified and structurally characterized from the reaction of 6-methylpyridine-2-methanol (**1**) with a range of cobalt(II) salts under a variety of reaction conditions. A tetranuclear cubane, $[Co_4(\mathbf{1}–H)_4Cl_4(H_2O)_3(CH_3OH)]$, was isolated from the reaction of **1** with $CoCl_2·6H_2O$ and NaOH in MeOH, and a tetranuclear double cubane, $[Co_4(\mathbf{1}–H)_6(NO_3)_2]$, was isolated from the reaction of **1** with $Co(NO_3)_2·6H_2O$ and NEt_3 in MeOH. A bowl-shaped trinuclear complex, $[Co_3(\mathbf{1}–H)_3Cl_3(dmso)]$, which features a triply bridging dmso ligand, assembled upon mixing **1** and $CoCl_2·6H_2O$ in dmso. A 1-D coordination polymer, $[Co(\mathbf{1})_2(SO_4)]_\infty$, where the sulfate ligands bridge "$[Co(\mathbf{1})_2]$" units in a μ^2:η^1 fashion to build up the polymer structure, was isolated from the reaction of **1** with $CoSO_4·7H_2O$. The reaction of the structurally related ligand 8-hydroxyquinaldine (**2**) with a mixture of $CoCl_2·6H_2O$ and $Co(OAc)_2·4H_2O$ lead to the formation of the tetranuclear double cubane, $[Co_4(\mathbf{2}–H)_6Cl_2]$. Temperature-dependent magnetic measurements have also been performed for these five complexes along with the hydrogen-bonded helicate $[Co_2(\mathbf{1})_2(\mathbf{1}–\mathbf{H})_2]$. The hydrogen bonds of the helicate mediate antiferromagnetic interactions between the cobalt(II) centers ($J = –3.18(9)$ cm^{-1}, $g = 2.25(2)$). The sulfate bridging ligands of $[Co(\mathbf{1})_2(SO_4)]_\infty$ are poor mediators of magnetic exchange. The Co(II) centers in the double-cubane complexes $[Co_4(\mathbf{1}–\mathbf{H})_6(NO_3)_2]$ and $[Co_4(\mathbf{2}–\mathbf{H})_6Cl_2]$ are strongly antiferromagnetically coupled to each other at low temperature to give an $S = 0$ ground state. $[Co_4(\mathbf{1}–\mathbf{H})_4Cl_4(H_2O)_3(MeOH)]$ exhibits rather complicated magnetic behavior; however, we did not observe any evidence for single-molecule magnetism as was seen for structurally related complexes.

Introduction

One domain of coordination chemistry which has flourished in recent years is the synthesis of complex polynuclear architectures via self-assembly processes involving suitably designed ligands and transition metal ions. We have been interested in the use of very simple building blocks for the self-assembly of metallo-supramolecular architectures, and we have recently focused on the use of simple pyridine-alcohol ligands.[1,2] As shown in Scheme 1, dinuclear double-stranded helicates self-assemble from mixtures of the commercially available ligand 6-methyl-pyridine-2-methanol (**1**) and a range of CoX_2 salts (X = halide, NO_3, SCN). The ligand strands in these helicates are built up using hydrogen bonding and are constructed as part of the overall self-assembly process. It can thus be seen that the synthesis of these helicates is a very straightforward process, and it is therefore amenable to a systematic investigation of the factors which control the outcome of this process.

In the present manuscript, we report our investigations into the reaction of ligands **1** and **2** with a range of cobalt(II) salts under a variety of experimental conditions. We have

* To whom correspondence should be addressed. E-mail: s.telfer@massey.ac.nz.
† JST ERATO Kuroda Chiromorphology Project.
‡ University of Tokyo.
§ Simon Fraser University.
# Current address: Institute of Fundamental Sciences—Chemistry, Massey University, Palmerston North, New Zealand.

(1) Telfer, S. G.; Sato, T.; Kuroda, R. *Angew. Chem., Int. Ed.* **2004**, *43*, 581−4.
(2) Telfer, S. G.; Kuroda, R. *Chem. Eur. J.* **2005**, *11*, 57−68.

10.1021/ic0517218 CCC: $33.50
Published on Web 04/28/2006

Scheme 1. Formation of Dinuclear Double-stranded Helicates from the Reaction of **1** with CoX_2 Salts[1,2] and the Structure of Ligands **2**−**4**

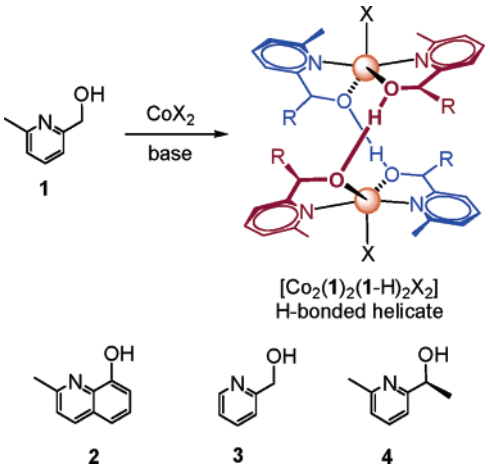

found that the self-assembly of hydrogen-bonded helicates proceeds only with certain cobalt(II) salts under a strictly limited set of conditions. Outside the borders of this regime, for example with added bases, different counteranions, or slightly modified ligands, the assembly of hydrogen-bonded helicates is diverted to the formation of alternative products. These products are notable for their diverse structures: in addition to helicates, we have characterized 1-D chains, bowls, and cubanes in the solid state. This work highlights the remarkable versatility of the coordination and supramolecular chemistry of simple pyridine-alcohol ligands. In addition to these important aspects of structural control, there is great current interest in exploring the magnetic properties of transition-metal clusters.[3] In particular, it is generally recognized that metal clusters with a large magnetic anisotropy are a prerequisite for single-molecule magnet behavior,[4] and clusters containing cobalt(II) centers, which generally show significant single-ion anisotropy, may show promise in this respect.[5,6] Hence, the magnetic properties of the reported cobalt(II) complexes are also presented in detail.

In addition to our investigations into the formation of hydrogen-bonded helicates from **1**, scattered reports concerning the coordination chemistry of this ligand exist in the literature. The thermodynamic stability constants of the $[Cu(\mathbf{1})]^{2+}$ and $[Cu(\mathbf{1})_2]^{2+}$ complexes have been determined potentiometrically,[7] and the $[Cu(\mathbf{1}-H)(OAc)]_2$ dimer has been structurally characterized.[8] Also, Zn(II)−thiolate complexes of this ligand have been used as structural models of alcoholdehydrogenase,[9] and the magnetic behavior of polynuclear Mn and Fe(III) complexes containing **1** has been investigated.[10,11] The parent ligand, pyridine-2-methanol (**3**), has been particularly well studied; this ligand exhibits a rich coordination chemistry and forms a diverse range of structures including mononuclear,[12] dinuclear,[13] and polynuclear complexes[6,14] and coordination polymers.[15]

Results and Discussion

Reaction of 1 with $CoCl_2$ and $Co(NO_3)_2$ in the Presence of Added Base. The synthesis of the hydrogen-bonded helicate $[Co_2(\mathbf{1})_2(\mathbf{1}-H)_2X_2]$ (Scheme 1) simply involves combining **1** and CoX_2 (4/1 ratio, X = Cl, Br, NO_3, etc.) in MeOH.[1,2] In this process, compound **1** acts as both a ligand and the requisite base. We also explored the use of alternative bases such as OAc^-, OH^-, and NEt_3; however we found that these bases led to the formation of mixtures of crystalline products which, on the basis of visual inspection, appeared to be the helicate along with varying amounts of a second product. In an effort to identify these products, we focused on two particular cases, viz., the reaction of **1** with $CoCl_2 \cdot 6H_2O$ and NaOH and the reaction of **1** with $Co(NO_3)_2 \cdot 6H_2O$ and NEt_3. In both cases we were able to find reaction conditions which led to the exclusive formation of the "non-helicate" products, and we were able to isolate and characterize these products.

In the first case, the reaction of **1** with $CoCl_2 \cdot 6H_2O$ and NaOH in MeOH, X-ray crystallography showed that the rose-colored crystalline product was $[Co_4(\mathbf{1}-H)_4Cl_4(H_2O)_3(MeOH)]$ (Figure 1). The four cobalt(II) ions are located at the vertexes of a cube with the triply bridging oxygen atoms of the four deprotonated $(\mathbf{1}-H)^-$ ligands occupying the remaining four vertexes. The pyridyl groups of two $(\mathbf{1}-H)^-$ ligands extend outward from opposite faces of the cubane in a parallel arrangement with a spacing of around 3.6 Å. This indicates that $\pi-\pi$ interactions may stabilize the complex. One chloro and one H_2O ligand extend outward from three of the remaining faces, while a chloro and a MeOH ligand occupy the final face of the cubane.

In the second case, the reaction of **1** with $Co(NO_3)_2 \cdot 6H_2O$ and NEt_3 in MeOH, the non-helicate product was shown to be $[Co_4(\mathbf{1}-H)_6(NO_3)_2]$ (Figure 2). This tetranuclear complex crystallizes in the space group $P\bar{1}$ and adopts a face-shared double cubane structure which has two missing vertexes. The

(3) (a) Beltran, L. M. C.; Long, J. R. *Acc. Chem. Res.* **2005**, *38*, 325−34. (b) Ruiz, E. *Struct. Bonding* **2004**, *113*, 71−102. (c) Thompson, L. K. *Coord. Chem. Rev.* **2002**, *233*, 193−206. (c) Winpenny, R. E. P. *Chem. Soc. Rev.* **1998**, *27*, 447−52.
(4) Gatteschi, D.; Sessoli, R. *Angew. Chem., Int. Ed.* **2003**, *42*, 268−97.
(5) (a) Murrie, M.; Teat, S. J.; Stoeckli-Evans, H.; Güdel, H. U. *Angew. Chem., Int. Ed.* **2003**, *42*, 4653−6. (b) Song, Y.; Zhang, P.; Ren, X.-M.; Shen, X.-F.; Li, Y.-Z.; You, X.-Z. *J. Am. Chem. Soc.* **2005**, *127*, 3708−9. (c) Karasawa, S.; Zhou, G.; Morikawa, H.; Koga, N. *J. Am. Chem. Soc.* **2003**, *125*, 13676−7.
(6) Yang, E.-C.; Hendrickson, D. N.; Wernsdorfer, W.; Nakano, M.; Zakharov, L. N.; Sommer, R. D.; Rheingold, A. L.; Ledezma-Gairaud, M.; Christou, G. *J. Appl. Phys.* **2002**, *91*, 7382−4.
(7) Lane, T. J.; Kanadathil, A. J.; Rosalie, S. M. *Inorg. Chem.* **1964**, *3*, 487−90.
(8) Cheng, S.-C.; Wei, H.-H. *Inorg. Chim. Acta* **2002**, *340*, 105−13.
(9) Mueller, B.; Schneider, A.; Tesmer, M.; Vahrenkamp, H. *Inorg. Chem.* **1999**, *38*, 1900−7.
(10) Canada-Vilalta, C.; Rumberger, E.; Brechin, E. K.; Wernsdorfer, W.; Folting, K.; Davidson, E. R.; Hendrickson, D. N.; Christou, G. *J. Chem. Soc., Dalton Trans.* **2002**, 4005−10.
(11) Yoo, J.; Yamaguchi, A.; Nakano, M.; Krzystek, J.; Streib, W. E.; Brunel, L.-C.; Ishimoto, H.; Christou, G.; Hendrickson, D. N. *Inorg. Chem.* **2001**, *40*, 4604−16.
(12) (a) Yilmaz, V. T.; Guney, S.; Andac, O.; Harrison, W. T. A. *Polyhedron* **2002**, *21*, 2393−402. (b) Suzuki, Y.; Tomizawa, H.; Miki, E. *Inorg. Chim. Acta* **1999**, *290*, 36−43.
(13) Yilmaz, V. T.; Hamamci, S.; Thone, C. *Polyhedron* **2004**, *23*, 841−8.
(14) (a) Harden, N. C.; Bolcar, M. A.; Wernsdorfer, W.; Abboud, K. A.; Streib, W. E.; Christou, G. *Inorg. Chem.* **2003**, *42*, 7067−76, (b) Brechin, E. K.; Knapp, M. J.; Huffman, J. C.; Hendrickson, D. N.; Christou, G. *Inorg. Chim. Acta* **2000**, *297*, 389−99.
(15) Ito, M.; Onaka, S. *Inorg. Chim. Acta* **2004**, *357*, 1039−46.

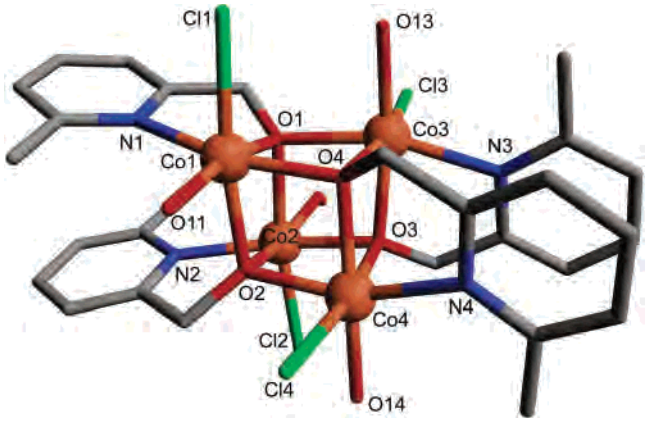

Figure 1. X-ray crystal structure of $[Co_4(\mathbf{1}-H)_4Cl_4(H_2O)_3(MeOH)]$. H atoms are omitted for clarity. Selected distances (Å): Co(1)−O(1) = 2.034(4); Co(2)−O(2) = 2.071(4); Co(3)−O(3) = 2.029(4); Co(4)−O(4) = 2.084(4); Co(1)−N(1) = 2.169(5); Co(2)−N(2) = 2.156(5); Co(3)−N(3) = 2.191(5); Co(4)−N(4) = 2.174(5); Co(1)−Cl(1) = 2.505(2); Co(2)−Cl(2) = 2.465(2); Co(3)−Cl(3) = 2.476(2); Co(4)−Cl(4) = 2.483(2). Selected angles (deg): Co(1)−O(1)−Co(3) = 100.0(2); Co(3)−O(4)−Co(1) = 97.0(2); Co(1)−O(2)−Co(4) = 97.6(2); Co(1)−O(4)−Co(4) = 100.3(2).

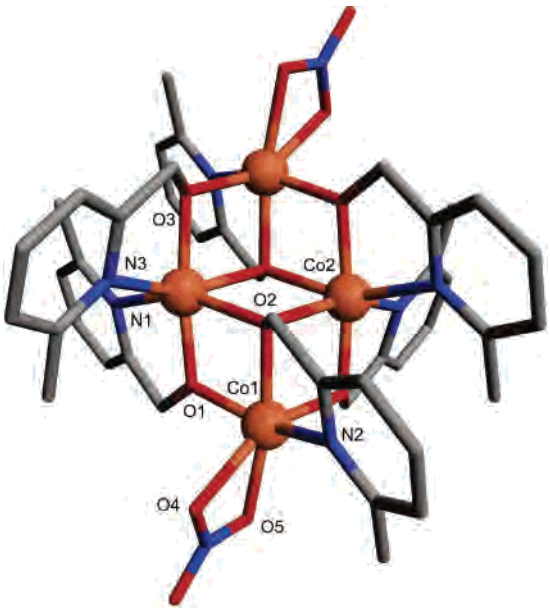

Figure 2. X-ray crystal structure of $[Co_4(\mathbf{1}-H)_6(NO_3)_2]$. H atoms are omitted for clarity. Selected distances (Å): Co(1)−O(1) = 1.987(5); Co(1)−O(2) = 2.097(5); Co(1)−N(2) = 2.168(6); Co(1)−O(4) = 2.241(5); Co(1)−O(5) = 2.195(5); Co(2)−O(1) = 1.975(5); Co(2)−O(3) = 2.030(5); Co(2)−N(1) = 2.216(6); Co(2)−N(3) = 2.180(6). Selected angles (deg): O(1)−Co(1)−O(2) = 80.1(2); Co(1)−O(1)−Co(2) = 106.4(2); Co(1)−O(2)−Co(2) = 92.5(2); N(1)−Co(2)−O(1) = 78.5(2); O(1)−Co(2)−O(2) = 78.0(2); O(2)−Co(2)−O(2′) = 80.3(2).

crystallographic inversion center relates the two halves of the cluster. Two of the cobalt(II) centers are coordinated to the pyridine rings of two $(\mathbf{1}-H)^-$ ligands and four bridging O atoms, while the other two are coordinated to one pyridine moiety, one bidentate NO_3^- ligand, and three bridging O atoms. Thus, the oxygen donor atoms of the $(\mathbf{1}-H)^-$ ligands bridge either two or three metal centers to build up the defect double-cubane structure.

Reaction of 1 with $CoCl_2$ and NEt_3 in dmso. In the course of investigating the influence of the solvent and added base on the assembly of $[Co_2(\mathbf{1})_2(\mathbf{1}-H)_2Cl_2]$ helicates, we

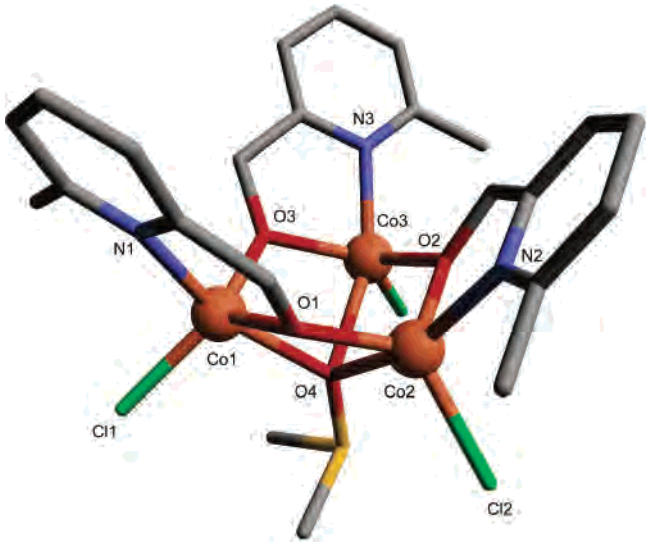

Figure 3. X-ray crystal structure of $[Co_3(\mathbf{1}-H)_3Cl_3(dmso)]$. H atoms are omitted for clarity. Selected distances (Å): Co(1)−O(1) = 1.955(3); Co(1)−N(1) = 2.124(4); Co(1)−O(4) = 2.320(3); Co(1)−Cl(1) = 2.283(1); O(1)−Co(2) = 1.962(3); Co−Co = 3.20−3.26. Selected angles (deg): Co(1)−O(1)−Co(2) = 111.3(1); Co(1)−O(4)−Co(2) = 88.3(1); N(1)−Co(1)−O(1) = 82.0(1).

reacted **1** with $CoCl_2$ and NEt_3 in dmso. A violet solution developed, and deep violet prismatic crystals could be isolated by adding MeOH to the reaction mixture. X-ray crystal structure analysis gave the structure shown in Figure 3: a bowl-shaped trinuclear complex, $[Co_3(\mathbf{1}-H)_3Cl_3(dmso)]$. The three cobalt(II) centers in this complex are linked in a triangular array by the three $(\mathbf{1}-H)^-$ ligands with an average Co···Co separation of 3.23 Å. The oxygen donors of the ligand bridge two cobalt(II) centers in a μ_2 fashion. The three chloro ligands coordinate in a terminal fashion on the outside of the bowl. Interestingly, a dmso molecule occupies the base of the bowl and is coordinated to the three Co(II) centers via its oxygen donor atom. A search of the Cambridge Crystallographic Database revealed that this coordination mode of a dmso ligand has been reported in the literature on only one previous occasion.[16] In this case, two dmso ligands were found to coordinate to the two faces of a trinuclear array of Hg(II) ions.[17] The IR spectrum of this complex exhibited a band at 1001 cm^{-1} which was attributed to the dmso S=O stretch (ν_{SO}). This stretch was found at 999 cm^{-1} in the IR spectrum of $[Co_3(\mathbf{1}-H)_3Cl_3(dmso)]$, and these values may be compared to the ν_{SO} value of free dmso of 1050 cm^{-1}.

The packing arrangement of $[Co_3(\mathbf{1}-H)_3Cl_3(dmso)]$ is also noteworthy, in particular the formation of a capsulelike dimer of the bowl-shaped complexes (Figure 4). Although the constituent complexes are chiral, they are related by a crystallographic inversion center (of the $P\bar{1}$ space group) to give a centrosymmetric capsule. A water molecule occupies the space within this capsule.

Reaction of 1 with $CoSO_4$. The formation of hydrogen-bonded helicates such as $[Co_2(\mathbf{1})_2(\mathbf{1}-H)_2Cl_2]$ can be moni-

(16) Cambridge Structural Database, version 5.26.
(17) Tikhonova, I. A.; Dolgushin, F. M.; Tugashov, K. I.; Petrovskii, P. V.; Furin, G. G.; Shur, V. B. *J. Organomet. Chem.* **2002**, *654*, 123−31.

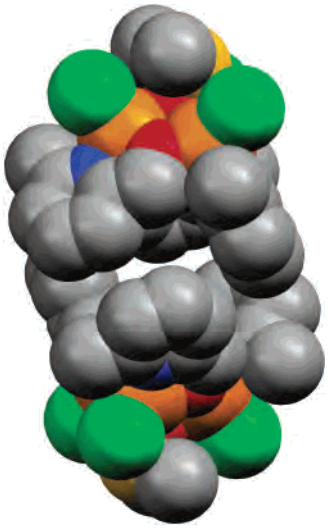

Figure 4. Diagram showing the formation of a capsule by two molecules of $[Co_3(\mathbf{1}-H)_3Cl_3(dmso)]$ in the solid state. A water molecule fills the void created by this capsule.

tored in solution by ^{1}H NMR spectroscopy when a solution of $CoCl_2 \cdot 6H_2O$ is titrated into a solution of **1** in CD_3OD. When the analogous titration was performed using $CoSO_4 \cdot 7H_2O$, the ^{1}H NMR spectrum displayed only several extremely broad and featureless peaks which suggested that the $[Co_2(\mathbf{1})_2(\mathbf{1}-H)_2(SO_4)_2]^{2-}$ helicate did not form. No trace of any fragments of the $[Co_2(\mathbf{1})_2(\mathbf{1}-H)_2(SO_4)_2]$ could be found in solution by ES-MS, indicating that its formation is highly disfavored. Pink crystals were observed to form from a solution of **1** and $CoSO_4 \cdot 7H_2O$ (2/1 ratio) in MeOH, and X-ray crystallography indicated that a 1-D coordination polymer, $[Co(\mathbf{1})_2SO_4]_\infty$, had formed (Figure 5).

Crystals of $[Co(\mathbf{1})_2SO_4]_\infty$ consist of infinite polymer chains which are built up from $[Co(\mathbf{1})_2]$ units which are linked by SO_4^{2-} ligands ligated to their axial sites. The SO_4^{2-} anions coordinate in a μ_2:η^1:η^1 fashion, bridging two metal centers via monodentate Co−O contacts. The alcohol groups of ligand **1** remain protonated. There are two crystallographically independent cobalt(II) centers, and the two **1** ligands of each metal center are related by inversion symmetry (space group $P\bar{1}$). The cobalt ions adopt a pseudo-octahedral geometry, and the metal−metal separation along the polymer chain is 6.036 Å. The close distances (ca. 3.3 Å) between pyridyl rings of neighboring chains and their parallel orientations suggest that interchain $\pi-\pi$ interactions may serve to stabilize the solid-state structure. There are several other examples of μ_2-sulfato-bridged cobalt(II) coordination polymers in the literature.[18]

Reaction of 8-Hydroxyquinaldine (2) with $CoCl_2$. The structural similarity of 8-hydroxyquinaldine (**2**) to ligand **1** prompted us to investigate the possible synthesis of the hydrogen-bonded helicate $[Co_2(\mathbf{2})(\mathbf{2}-H)_2Cl_2]$. To this end, ligand **2** was dissolved in CH_2Cl_2 and combined with a methanolic solution of $CoCl_2 \cdot 6H_2O$ and $Co(OAc)_2 \cdot 4H_2O$. Brown crystals could be isolated from the reaction mixture, and X-ray crystallography revealed the structure shown in Figure 6. The complex, $[Co_4(\mathbf{2}-H)_6Cl_2]$, has a defect double-cubane structure which is very similar to that of $[Co_4(\mathbf{1}-H)_6(NO_3)_2]$. Again, the complex crystallizes in the $P\bar{1}$ space group with the inversion center located at the center of the cluster. Two of the cobalt(II) ions coordinate to two deprotonated bidentate $(\mathbf{2}-H)^-$ ligands, while the other two metal centers bind one bidentate $(\mathbf{2}-H)^-$ ligand and one chloro ligand. The oxygen donor atoms of the $(\mathbf{2}-H)^-$ ligands bridge either two or three cobalt(II) centers to build up the cubane structure. The utility of ligand **2** for building up large polynuclear assemblies has been noted in the literature with tetranuclear cobalt(II) and nickel(II) cubane clusters,[19] and a tetranuclear cubane copper(I) cluster[20] having been reported.

Factors Influencing the Self-Assembly Process. The self-assembly of $[Co_2(\mathbf{1})_2(\mathbf{1}-H)_2X_2]$ helicates from ligand **1** and cobalt(II) salts proceeds only under a narrow well-defined set of reaction conditions. As discussed below, many factors disrupt the assembly of these helicates; for example, certain counteranions and solvents and the presence of added base lead to alternative products.

It appears that $[Co_2(\mathbf{1})_2(\mathbf{1}-H)_2X_2]$ helicates only form when X is a monoanionic ligand with a reasonably strong coordinating ability: the reaction of $Co(ClO_4)_2 \cdot 6H_2O$ with **1** does not lead to the formation of helicates (as the perchlorate anion is too weakly coordinating) nor does the reaction of $CoSO_4$ with **1** (as the sulfate anion carries a 2− charge). As described above, the actual product in this case is a sulfate-bridged coordination polymer.

The presence or absence of added base has a clear impact on the coordination chemistry of ligand **1**, apparently by controlling the coordination mode of the alcohol group. Under conditions of moderate basicity, $[Co_2(\mathbf{1})_2(\mathbf{1}-H)_2X_2]$ helicates are observed. These helicates are built up by hydrogen bonding between alcohol groups which are coordinated to different metal centers. In the presence of added bases, such as NaOH and NEt_3, high-nuclearity cubane-type clusters have a tendency to form. Such behavior is characteristic of ligand **1**[11] and related pyridine-alcohol ligands, such as **3**.[6,21] Under conditions of relatively high basicity, complete deprotonation of the coordinated alcohol moieties allows the oxygen centers to form one vertex of a cubane structure by bridging in a μ_3 mode. A counter-example to this general trend is observed when dmso is used as the solvent and NEt_3 as the base. Here, the trinuclear bowl-shaped structure $[Co_3(\mathbf{1}-H)_3Cl_3(dmso)]$ forms with the deprotonated oxygens of **1** bridging only two cobalt(II) centers and the dmso ligand playing a key structural role. In

(18) (a) Li, X.-H.; Chi, X.-X. *Acta Crystallogr. E* **2004**, *60*, m1301. (b) Ali, H. M.; Puvaneswary, S.; Ng, S. W. *Acta Crystallogr. E* **2005**, *61*, m474. (c) Dong, Y.-B.; Ma, J.-P.; Huang, R.-Q.; Liang, F.-Z.; Smith, M. D. *Dalton Trans.* **2003**, 1472−9. (d) Zhang, Y.-X. *Acta Crystallogr. E* **2004**, *60*, m30. (e) Carlucci, L.; Ciani, G.; Proserpio, D. M.; Rizzato, S. *CrystEngComm* **2003**, *5*, 190. (f) Carlucci, L.; Ciani, G.; Proserpio, D. M. *Chem. Commun.* **2003**, 380−1. (g) Vreshch, V. D.; Chernega, A. N.; Howard, J. A. K.; Sieler, J.; Domasevitch, K. V. *Dalton Trans.* **2003**, 1707−11.

(19) Aromi, G.; Batsanov, A. S.; Christian, P.; Helliwell, M.; Roubeau, O.; Timco, G. A.; Winpenny, R. E. P. *Dalton Trans.* **2003**, 4466−71.

(20) Pasquali, M.; Fiaschi, P.; Floriani, C.; Zanazzi, P. F. *Chem. Commun.* **1983**, 613−4.

(21) Escuer, A.; Font-Bardia, M.; Kumar, S. B.; Solans, X.; Vicente, R. *Polyhedron* **1999**, *18*, 909−14.

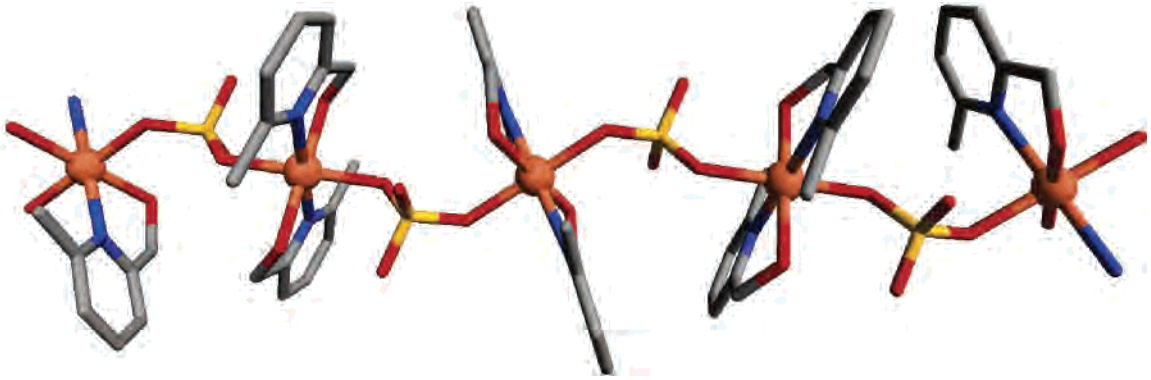

Figure 5. X-ray crystal structure of $[Co(\mathbf{1})_2SO_4]_\infty$. H atoms are omitted for clarity (orange = Co, red = O, blue = N, yellow = S). Selected distances (Å): $Co-O^{sulfate} = 2.099(1)$, 2.095(1); $Co-O^{py} = 2.112(1)$; Co−N = 2.186(2), 2.178(2). Selected angles (deg): $Co-O^{sulfate}-S = 125.96(8)$, 131.00(8); $O^{py}-Co-N^{py} = 77.05(6)$, 77.08(6); $(Co)O^{sulfate}-S-O^{sulfate}(Co) = 108.47(8)$.

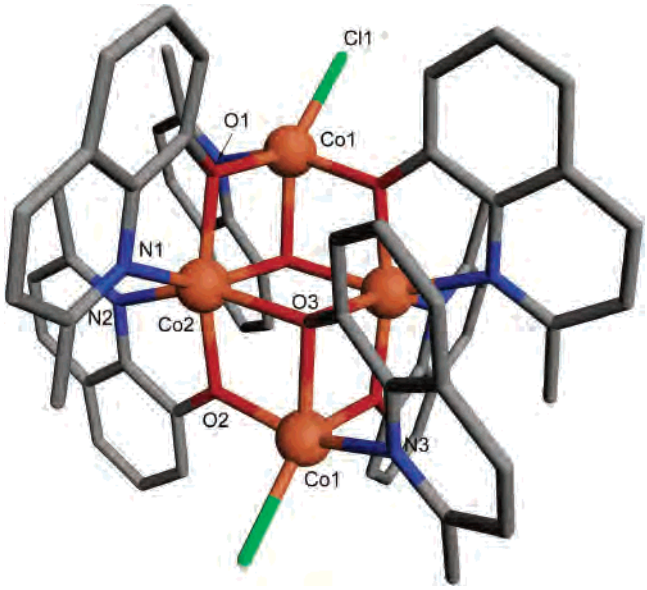

Figure 6. X-ray crystal structure of $[Co_4(\mathbf{2}-H)_6Cl_2]$. H atoms are omitted for clarity. Selected distances (Å): Co(1)−O(2) = 2.003(3); Co(1)−O(3) = 2.107(3); Co(1)−Cl(1) = 2.289(2); Co(1)−N(3) = 2.102(5); Co(1)−Co(2) = 3.326; Co(2)−O(2) = 2.003(3); Co(2)−O(3) = 2.242(4); Co(2)−N(1) = 2.120(5); Co(2)−N(2) = 2.129(4). Selected angles (deg): Co(1)−O(2)−Co(2) = 108.2(2); Co(1)−O(3)−Co(2) = 93.0(1); O(3)−Co(1)−N(3) = 77.7(2); Co(2)−O(3)−Co(2′) = 98.7(1).

the absence of added base, ligand **1** may coordinate without deprotonation, as observed for $[Co(\mathbf{1})_2SO_4]_\infty$.

We have previously observed that minor changes to the structure of the pyridyl alcohol ligand, for example, replacing the ortho methyl group of **1** by H or Br, can disrupt the formation of hydrogen-bonded helicates.[2] We were interested in observing the outcome of the reaction using ligand **2**, and we found that a mixture of **2**, $CoCl_2$, and $Co(OAc)_2$ led to the production of $[Co_4(\mathbf{2}-H)_6Cl_2]$. We initially assumed that this ligand was completely unsuitable for the formation of hydrogen-bonded helicates; however, during the course of this work, we came across literature results describing the formation of hydrogen-bonded dimers of nickel(II) complexes, $[Ni_2(\mathbf{2})_3(\mathbf{2}-H)_3]$ (Figure S1).[22,23] Although these complexes were not described in these terms, they may be viewed as helical structures and thus as triple-stranded analogues of our $[Co_2(\mathbf{1})_2(\mathbf{1}-H)_2X_2]$ hydrogen-bonded helicates. This prompted us to investigate the possibility of preparing $[Co_2(\mathbf{2})_3(\mathbf{2}-H)_3]$ helicates using the experimental conditions reported for the nickel(II) helicates $(Ni(ClO_4)_2\cdot 6H_2O$ and **2** (1/5 ratio) in ethanol). We found, however, that the reaction of $Co(ClO_4)_2\cdot 6H_2O$ and **2** under these conditions led instead to the formation of a trinuclear cluster $[Co_3(\mathbf{2}-H)_6]$.[24] Interestingly, the papers which described the original Ni(II) dimers reported that a Ni/**2** ratio of 1/5 is crucial for the formation of the hydrogen-bonded structures, with greater amounts of nickel(II) leading to other products. From these results, we may identify a further two factors which have a decisive impact on the outcome of the self-assembly processes involving simple pyridine-alcohol ligands and metal salts: the nature of the metal ion and the metal-to-ligand ratio. We are examining the former point in detail and hope to report our results concerning the reaction of ligands **1**−**4** with nickel(II), copper(II), and zinc(II) salts soon.

Magnetic properties of $[Co(\mathbf{1})_2SO_4]_\infty$. The temperature dependence of the molar magnetic susceptibility (χ_M) of the Co(II)−SO_4 bridged polymer $[Co(\mathbf{1})_2SO_4]_\infty$ was studied in the temperature range of 300−1.8 K. The magnetic susceptibility (χ_M) and the product of the susceptibility with temperature ($\chi_M T$) are shown in Figure 7. The $\chi_M T$ value observed at 300 K (3.03 emu K mol^{-1}) is larger than the value for a spin-only $S = 3/2$ system (1.875 emu K mol^{-1}). This is as expected for octahedral high-spin cobalt(II) ions, which have a large first-order orbital contribution to the magnetic moment.[25] As the temperature decreases, $\chi_M T$ decreases and reaches a value of 0.92 emu K mol^{-1} at 1.8 K. This decrease is indicative of a combination of weak interactions mediated along the chains by the SO_4^{2-} units, as well as the single-ion effects of the cobalt(II) centers.[26]

(22) (a) Yuchi, A.; Murakami, H.; Shiro, M.; Wada, H.; Nakagawa, G. *Bull. Chem. Soc. Jpn.* **1992**, *65*, 3362−73. (b) Kiriyama, H.; Fukuda, T.; Yamagata, Y.; Sekido, E. *Acta Crystallogr. C* **1985**, *41*, 1441. (c) Kiriyama, H.; Yamagata, Y.; Suzuki, K. *Acta Crystallogr. C* **1986**, *42*, 785. (d) Kiriyama, H.; Yamagata, Y.; Yonetani, K.; Sekido, E. *Acta Crystallogr. C* **1986**, *42*, 56.
(23) A related tridentate ligand leads to dinuclear double-stranded hydrogen-bonded helicates: Petkova, E. G.; Lampeka, R. D.; Gorichko, M. V.; Domasevitch, K. V. *Polyhedron* **2000**, *20*, 747.
(24) Telfer, S. G. Unpublished observations.
(25) Kahn, O. *Molecular Magnetism*; VCH: Weinheim, Germany, 1993.
(26) Leznoff, D. B.; Xue, B.-Y.; Stevens, C. L.; Storr, A.; Thompson, R. C.; Patrick, B. O. *Polyhedron* **2001**, *20*, 1247−54.

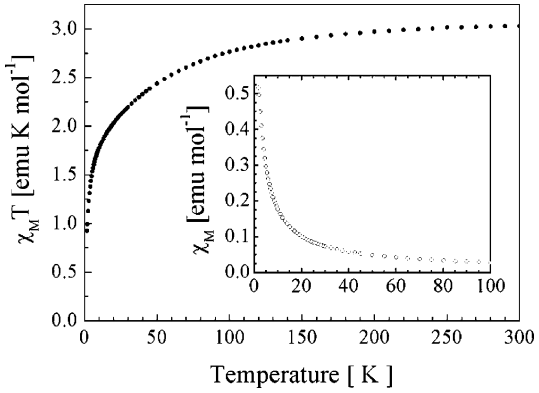

Figure 7. Temperature dependence of $\chi_M T$ for $[Co(\mathbf{1})_2SO_4]_\infty$. The inset shows the magnetic susceptibility (χ_M) at low temperature.

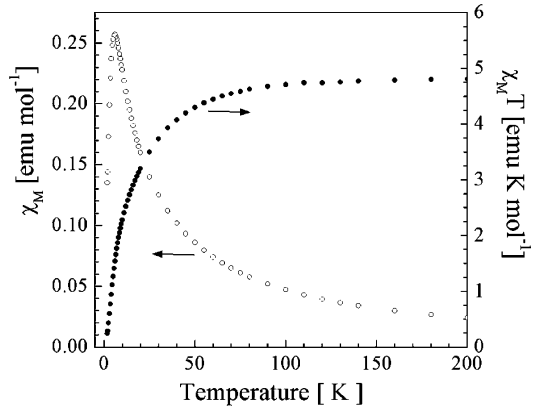

Figure 8. Temperature dependence of χ_M (○) and $\chi_M T$ (●) for $[Co_2(\mathbf{1})_2(\mathbf{1}-H)_2Cl_2]$.

The simultaneous presence of single-ion effects and weak coupling severely complicates modeling of these data.[27,28]

Although the large drop in $\chi_M T$ indicates that some coupling is operative, there is no maximum observed down to 1.8 K in the temperature dependence of χ_M; thus, the single-ion effects dominate the magnetic behavior. Since any antiferromagnetic interactions between the cobalt(II) centers are very weak, the SO_4^{2-} ion is clearly a poor mediator of magnetic exchange in $[Co(\mathbf{1})_2SO_4]_\infty$. This result correlates well with the very small (<1 cm^{-1}) J couplings, determined using the Bleaney−Bowers model, for the $Cu(\mu_2\text{-}SO_4)_2Cu$ complexes, for which single-ion effects are absent.[29]

Magnetic Properties of $[Co_2(\mathbf{1})_2(\mathbf{1}-H)_2Cl_2]$. The temperature dependence of χ_M and $\chi_M T$ for the hydrogen-bonded helicate $[Co_2(\mathbf{1})_2(\mathbf{1}-H)_2Cl_2]$ are shown in Figure 8. At 300 K, $\chi_M T$ is 4.77 emu K mol^{-1}, which is higher than the value expected for two isolated $S = 3/2$ spin-only centers (3.75 emu K mol^{-1}). In $[Co_2(\mathbf{1})_2(\mathbf{1}-H)_2Cl_2]$, the cobalt(II) centers have a five-coordinate geometry, therefore the orbital degeneracy is reduced in comparison to the octahedral cobalt(II) centers. As a consequence, the orbital contribution to the magnetic moment is also diminished.[30] As the temperature decreases, the $\chi_M T$ value remains constant until the temperature reaches ca. 75 K, below which $\chi_M T$ decreases rapidly to a value of 0.24 emu K mol^{-1} at 1.8 K. The maximum observed in the temperature-dependent magnetic susceptibility, in the vicinity of 6 K, is indicative of antiferromagnetic coupling occurring between the two cobalt(II) centers. The data were fit to a dimer (with $S = 3/2$ per cobalt) using an isotropic Heisenberg Hamiltonian ($H = -JS_1S_2$), thereby neglecting any orbital contribution or zero-field splitting effects. An approximate fit was obtained ($R^2 = 0.991$), with a coupling constant, J, of $-3.18(9)$ cm^{-1} and a g value of 2.25(2). More detailed modeling studies to account for the single-ion effects were not attempted. The value of J obtained above is comparable to that reported for other coupled cobalt(II) dimers.[28,30] The antiferromagnetic coupling between the cobalt(II) centers in the helicate is stronger than in the SO_4-linked polymer; magnetic interactions are likely mediated by the tight hydrogen bonding (O−O distance = 2.42 Å) across the Co−(OHO)−Co bridges.[1,31,32] Significant ferromagnetic and antiferromagnetic interactions at low temperature are known to be mediated by hydrogen bonds in a range of systems.[33]

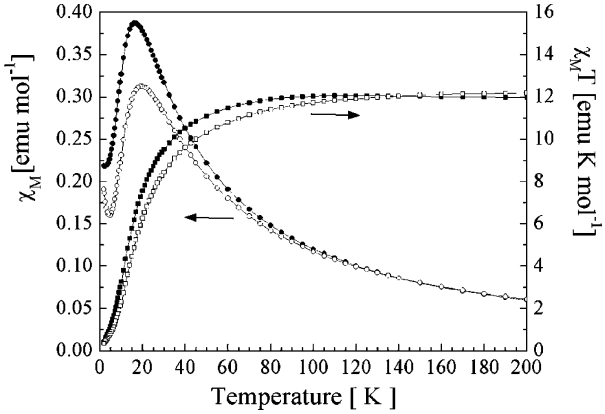

Figure 9. Temperature dependence of χ_M and $\chi_M T$ for $[Co_4(\mathbf{1}-H)_6(NO_3)_2]$ (● and ■, respectively) and $[Co_4(\mathbf{2}-H)_6Cl_2]$ (○ and □, respectively). Solid lines added to aid visualization only.

Magnetic Properties of $[Co_4(\mathbf{1}-H)_6(NO_3)_2]$ and $[Co_4(\mathbf{2}-H)_6Cl_2]$. The two tetranuclear complexes $[Co_4(\mathbf{1}-H)_6(NO_3)_2]$ and $[Co_4(\mathbf{2}-H)_6Cl_2]$ have very similar defect double-cubane structures, and they exhibit similar magnetic behavior (Figure 9). At 300 K, the $\chi_M T$ values observed per cluster are 11.23 and 12.22 emu K mol^{-1} for $[Co_4(\mathbf{1}-H)_6(NO_3)_2]$ and $[Co_4(\mathbf{2}-H)_6Cl_2]$, respectively. These values are consistent

(27) Sun, J.-S.; Zhao, H.; Ouyang, X.; Clerac, R.; Smith, J. A.; Clemente-Juan, J. M.; Gomez-Garcia, C.; Coronado, E.; Dunbar, K. R. *Inorg. Chem.* **1999**, *38*, 5841−55.
(28) Sakiyama, H.; Ito, R.; Kumagai, H.; Inoue, K.; Sakamoto, M.; Nishida, Y.; Yamasaki, M. *Eur. J. Inorg. Chem.* **2001**, 2027−32.
(29) Telfer, S. G.; Sato, T.; Harada, T.; Kuroda, R.; Lefebvre, J.; Leznoff, D. B. *Inorg. Chem.* **2004**, *43*, 6168−76.
(30) Beckmann, U.; Brooker, S.; Depree, C. V.; Ewing, J. D.; Moubaraki, B.; Murray, K. S. *Dalton Trans.* **2003**, 1308−13.
(31) Serna, Z. E.; Urtiaga, M. K.; Barandika, M. G.; Cortés, R.; Martin, S.; Lezama, L.; Arriortua, M. I.; Rojo, T. *Inorg. Chem.* **2001**, *40*, 4550−5.
(32) King, P.; Clérac, R.; Wernsdorfer, W.; Anson, C. E.; Powell, A. K. *Dalton Trans.* **2004**, 2670−6.
(33) (a) Ren, X.; Chen, Y.; He, C.; Gao, S. J. *Dalton Trans.* **2002**, 3915−8. (b) Papoutsakis, D.; Kirby, J. P.; Jackson, J. E.; Nocera, D. G. *Chem. Eur. J.* **1999**, *5*, 1474−80. (c) Plass, W.; Pohlmann, A.; Rautengarten, J. *Angew. Chem., Int. Ed.* **2001**, *40*, 4207−10. (d) Isele, K.; Broughton, V.; Matthews, C. J.; Williams, A. F.; Bernardinelli, G.; Franz, P.; Decurtins, S. *J. Chem. Soc., Dalton Trans.* **2002**, 3899−905. (e) Desplanches, C.; Ruiz, E.; Alvarez, S. *Chem. Commun.* **2002**, 2614−5. (f) Wernsdorfer, W.; Allaga-Alcade, N.; Hendrickson, D. N.; Christou, G. *Nature* **2002**, *416*, 406−9.

Scheme 2. Spin-Diagram of $[Co_4(\mathbf{1}-H)_6(NO_3)_2]$ and $[Co_4(\mathbf{2}-H)_6Cl_2]$

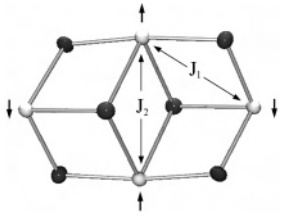

with four uncoupled octahedral Co(II) centers; each metal center in the cluster has an environment similar to that in the $[Co(\mathbf{1})_2SO_4]_\infty$ system ($\chi_M T_{300K} = 3.03$ emu K mol^{-1}), hence the single-ion effects should be similar. For both complexes, $\chi_M T$ is relatively constant from 300 to 100 K and then decreases rapidly to 0.34 and 0.39 emu K mol^{-1} at 1.8 K for $[Co_4(\mathbf{1}-H)_6(NO_3)_2]$ and $[Co_4(\mathbf{2}-H)_6Cl_2]$, respectively. Maxima can be observed in the temperature-dependent magnetic susceptibility curve (χ_M) at 16.5 and 19.5 K for $[Co_4(\mathbf{1}-H)_6(NO_3)_2]$ and $[Co_4(\mathbf{2}-H)_6Cl_2]$, respectively. The drop in $\chi_M T$ to almost zero and the maximum in χ_M indicate that the Co(II) centers in these double-cubane complexes are strongly antiferromagnetically coupled to each other at low temperature to yield an $S = 0$ ground state. A spin-coupling diagram for the double-cubane structure is illustrated in Scheme 2, in which the two coupling pathways are represented by J_1 (around the edge) and J_2 (through the center).[35] The observed magnetic properties can be rationalized with the J_1 coupling being significantly antiferromagnetic and the central J_2 coupling being either ferromagnetic or negligible; if both J_1 and J_2 are negative, a spin-frustrated system would result. Minor bond length, angle, and ligand-field differences between the two clusters readily account for the slightly different maxima in χ_M for the two clusters. The slight increase observed below 4 K in the magnetic susceptibility curve for $[Co_4(\mathbf{2}-H)_6Cl_2]$ is likely the result of a very minor paramagnetic impurity.

The double-cubane structure adopted in $[Co_4(\mathbf{1}-H)_6(NO_3)_2]$ and $[Co_4(\mathbf{2}-H)_6Cl_2]$ is not an unusual motif, and the magnetic properties of several such cobalt(II) clusters have been studied. Both strongly ferromagnetically[31,32,34−36] and antiferromagnetically[34] coupled systems have been reported. The chemical nature of the mediating bridge, as expected, affects the observed magnetic interactions; in general, nitrogen-based donors such as bridging azido and cyanate groups all form ferromagnetic clusters. Table 1 compares the structural parameters of different defect double-cubane cobalt(II) clusters.

An examination of the bond lengths and angles between the cobalt(II) centers in the cluster for magnetostructural correlations does not reveal an obvious trend based on a single structural parameter, perhaps because of the wide range of ligands used to construct the clusters. The type of magnetic interactions mediated by the bridging atoms (X) is influenced by two main structural factors, the Co−X−Co angles and the Co−X bond lengths, which dictate the extent of possible orbital overlap. When the values reported for the different cobalt(II) clusters are compared, some general observations can be made. First, the through-cluster inner Co−X−Co angles (α in Scheme 3) generally range from 97.49 to 99.74°; such angles should favor ferromagnetic interactions because of the significant orbital orthogonality between the metal centers and the bridging atom.[37] Hence, the through-cluster J_2 value is most likely positive (i.e., ferromagnetic) or negligible for most clusters.

As a consequence of this invariance in the sign of J_2, the sign of J_1 becomes the key factor determining the overall magnetic properties of the clusters. Upon examination of Table 1, the clusters that show antiferromagnetic interactions are characterized by at least one large (>102°) Co−O−Co angle (β or γ in Scheme 3) coupled with short Co−O bonds (as in $[Co_4(\mathbf{2}-H)_6Cl_2]$ and $[Co_4(\mathbf{1}-H)_6NO_3]$); this situation favors orbital overlap and, as a consequence, an antiferromagnetic J_1 interaction. On the other hand, the ferromagnetically coupled clusters show, in general, smaller Co−O−Co angles, coupled with longer (on average) Co−O distances, yielding better orthogonality and a ferromagnetic J_1. The Co−X−Co angles allowing or preventing orbital overlap differ for nitrogen and oxygen bridging atoms. Thus, when X = N, the Co−N−Co angles are slightly larger (between 100 and 105°) than those for X = O, but they still favor ferromagnetic interactions.

The magnetic properties of the unique $[Co_4Cl_2(OC_2H_4OEt)_6]$ system,[34] which shows a mixture of ferro- and antiferromagnetic coupling, can be rationalized in terms of an antiferromagnetic J_2 attributable to a very short through-cluster Co−Co distance of 2.724 Å and a very acute through-cluster Co−O−Co angle of 78.46°; this coupling leads to complex spin-frustrated magnetic behavior regardless of the sign of J_1 (Scheme 2).

Magnetic Properties of $[Co_3(\mathbf{1}-H)_3Cl_3(dmso)]$. The temperature dependence of χ_M and $\chi_M T$ for the trinuclear $[Co_3(\mathbf{1}-H)_3Cl_3(dmso)]$ complex are shown in Figure 10. At 300 K, $\chi_M T$ has a value of 5.85 emu K mol^{-1} which is consistent with three isolated $S = 3/2$ five-coordinate cobalt(II) centers with a second-order orbital contribution to the magnetic moment. As the temperature decreases, $\chi_M T$ decreases and reaches a value of 0.30 emu K mol^{-1} at 1.8 K, indicative of dominant antiferromagnetic interactions in the complex. However, no maximum is observed in the temperature-dependent susceptibility curve. The interpretation of the magnetic properties of $[Co_3(\mathbf{1}-H)_3Cl_3(dmso)]$ is rather complicated because a triangular arrangement of metal centers naturally generates a spin-frustrated system.[38] Magnetic exchange between the cobalt(II) centers could potentially be mediated through the ligand **1,** the dmso oxygen atom, or both. If antiferromagnetic interactions were dominant, a ground state of $S = 1/2$ would reasonably be expected.

(34) Seisenbaeva, G.; Kritikos, M.; Kessler, V. G. *Polyhedron* **2003**, *22*, 2581−6.
(35) Papaefstathiou, G. S.; Escuer, A.; Raptopoulou, C. P.; Terzis, A.; Perlepes, S. P.; Vicente, R. *Eur. J. Inorg. Chem.* **2001**, 1567−74.
(36) Papaefstathiou, G. S.; Escuer, A.; Font-Bardia, M.; Perlepes, S. P.; Solans, X.; Vicente, R. *Polyhedron* **2002**, *21*, 2027−32.
(37) Hatfield, W. E. In *Magneto-Structural Correlations in Exchange Coupled Systems*; Willet, R. D., Gatteschi, D., Kahn, O., Eds.; Reidel: Dordrecht, The Netherlands, 1984; p 555.
(38) Greedan, J. E. *J. Mater. Chem.* **2001**, *11*, 37−53.

Table 1. Comparison of Bond Lengths and Angles (Scheme 3) in Different Defect Double-Cubane Cobalt(II) Clusters (where F = ferromagnetic interactions, AF = antiferromagnetic interactions, and X = O unless otherwise stated)[a]

		α (deg)	β (deg)	γ (deg)	inner Co−Co (Å)	outer Co−Co (Å)	Co−X_{out} (Å)	Co−X_{in} (Å)	ref
$[Co_4(\mathbf{2}-H)_6Cl_2]$	AF	98.71	108.16 104.27	96.99 92.97	3.380	3.236 3.155	2.003 1.992 1.984 2.013	2.241 2.108 2.213 2.241	this work
$[Co_4(\mathbf{1}-H)_6(NO_3)_2]$	AF	99.74	100.8 106.4	92.54 95.41	3.337	3.085 3.174	1.974 1.987 1.975 2.030	2.097 2.172 2.193	this work
$[Co_2(dpk{\cdot}OH)(dpk{\cdot}CH_3O)(N_3)(H_2O)]_2(BF_4)_2{\cdot}4H_2O$ (and isomorphous NCO)	F	98.7	97.9 102.3 (X = N)	96.7 98.9	3.169	3.156 3.291	2.027 2.156 2.132 (X = N)	2.189 2.142 2.034	31
$[Co_2(dpk{\cdot}OH)\ (dpk{\cdot}CH_3O)(NCO)_2]_2$	F	98.3	99.6 101.7 (X = N)	98.5 97.2	3.144	3.238 3.283	2.193 2.046 2.088 (X = N) 2.146 (X = N)	2.025 2.133 2.244	31
$[Co_4Cl_2(OC_2H_4OEt)_6]$	F and AF	78.46	103.78 112.96	90.48 100.63	2.7238	3.062 3.235	1.975 2.019 1.871 1.904	2.098 2.206 2.105	34
$[Co_4(OMe)_2(acac)_6(MeOH)_2]$	AF	97.49	97.33 95.89	101.19 102.17	3.139	3.212 3.185	2.081 2.084 2.242 2.157	2.091 2.084 2.037	34
$[Co_4(\mu_{1,1}\text{-}N_3)_2(N_3)_2\{(py)_2C(OH)O\}_2\{(py)_2C(OCH_3)O\}_2]{\cdot}2H_2O$	F	98.2	98.1 104.5 (X = N)	96.7 96.8	3.172	3.286 3.184	2.063 2.099 (X = N) 2.151 2.058 (X = N)	2.030 2.165 2.227	35
$[Co_4(N_3)_2(O_2CPh)_2\{(py)_2C(OH)O\}_4]{\cdot}2DMF$	F	97.8	101.1 (X = N) 98.5	97.4 96.2	3.1442	3.2897 3.1581	2.012 2.158 2.103 2.154	2.225 2.015 2.155	36
$[Co_4(\mu_3\text{-}OH)_2(N_3)_2(H_2O)_6(ntp)_2]{\cdot}2H_2O$	F	98.69	96.33 96.39	101.43 100.79	3.1342	3.2026 3.1884	2.110 2.134 2.165 2.167	2.072 2.065 2.066	32

[a] acac = 2,4-pentanedionato; DMF = *N*,*N*-dimethylformamide; dpk = di-2-pyridyl ketone; ntp = nitrilotripropionate; py = pyridine.

Scheme 3. Angles and Distances of Defect Double-Cubane Cobalt Clusters Referred to in Table 1

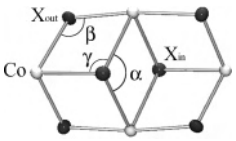

In this case, $\chi_M T$ should plateau at 0.375 emu K mol^{-1} at low temperatures[39] which is close to the observed value at 1.8K. However, a small field-dependence was also observed for this system (Figure 10, inset), suggesting that a more complex spin-ladder diagram may be operative. A detailed theoretical treatment of a spin-frustrated trinuclear cobalt-(II) system, in which the metal centers are tetrahedrally coordinated, was recently reported.[39]

Magnetic Properties of $[Co_4(1-H)_4Cl_4(H_2O)_3(MeOH)]$. The magnetic properties of the tetranuclear cubane cluster $[Co_4(\mathbf{1}-H)_4Cl_4(H_2O)_3(MeOH)]$ (Figure 11) differ from that observed for the defect double-cubane clusters. In this complex, the cobalt(II) centers have octahedral geometries, thus a large orbital contribution to the magnetic moment can be expected. At 300 K, $\chi_M T$ is 12.41 emu K mol^{-1} per cluster, consistent with four noninteracting octahedral cobalt(II)

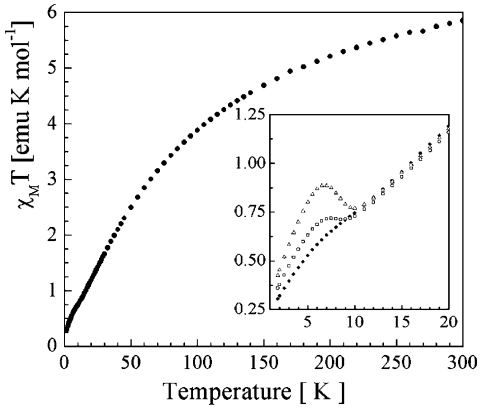

Figure 10. Temperature dependence of $\chi_M T$ measured for $[Co_3(\mathbf{1}-H)_3Cl_3(dmso)]$ (●). The inset shows the field dependence observed below 10 K under an external magnetic field of 50 Oe (△), 100 Oe (□), and 1000 Oe (●).

(39) Berry, J. F.; Cotton, F. A.; Liu, C. Y.; Lu, T.; Murillo, C. A.; Tsukerblat, B. S.; Villagran, D.; Wang, X. *J. Am. Chem. Soc.* **2005**, *127*, 4895−902.

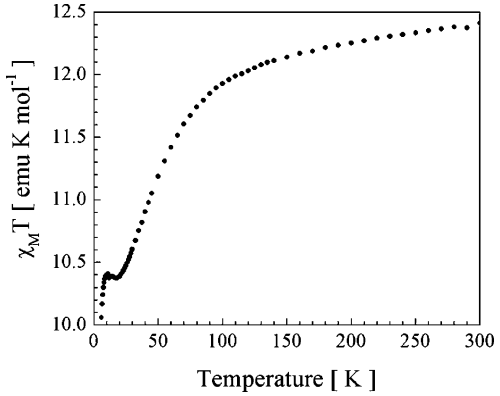

Figure 11. Temperature dependence of $\chi_M T$ for $[Co_4(\mathbf{1}-H)_4Cl_4(H_2O)_3(MeOH)]$ (●).

centers. As the temperature decreases, $\chi_M T$ decreases steadily until 17 K where it reaches a minimum value (10.38 emu K mol^{-1}). The $\chi_M T$ values increases, upon further cooling, to reach a maximum at 11 K, followed by a decrease to a final value of 10.06 emu K mol^{-1} at 1.8 K. A small field dependency in the temperature dependence of $\chi_M T$ was observed between 2 and 20 K.

This complex magnetic behavior of $[Co_4(\mathbf{1}-H)_4Cl_4(H_2O)_3(MeOH)]$ is similar to the data reported for another tetranuclear cubane, $[Co_4(\mathbf{3}-H)_4Cl_4(MeOH)_4]$;[6] however, the salient features of the curve for the former complex occur at much lower temperatures. Whereas $[Co_4(\mathbf{3}-H)_4Cl_4(MeOH)_4]$ behaves as a single-molecule magnet with a significant out-of-phase χ_M'' signal at 1.8 K,[6] there is no χ_M'' signal down to 1.8 K for $[Co_4(\mathbf{1}-H)_4Cl_4(H_2O)_3(MeOH)]$. The structures of the two cubane complexes are very similar with the only major differences being the presence of an ortho methyl group on ligand **1** in $[Co_4(\mathbf{1}-H)_4Cl_4(H_2O)_3(MeOH)]$ and the identity of the terminal ligands (MeOH versus MeOH/H_2O). The additional steric strain imposed by the ortho methyl group in $[Co_4(\mathbf{1}-H)_4Cl_4(H_2O)_3(MeOH)]$ appears to cause an elongation of most of the bond lengths compared to those of $[Co_4(\mathbf{3}-H)_4Cl_4(MeOH)_4]$: for example, the Co−Cl distances are notably longer (2.465(2)−2.505(2) vs 2.3758(9)−2.3827(8) Å).[6] This elongation of bond lengths, which presumably lowers all of the magnetic coupling interactions, along with the symmetry-lowering impact[40] of the mixed terminal ligands are likely factors that eliminate any single-molecule magnetism in $[Co_4(\mathbf{1}-H)_4Cl_4(H_2O)_3(MeOH)]$.

The magnetic properties of several other tetranuclear cobalt(II) cubanes have been reported; however, because of the difficulties associated with simultaneously modeling multiple magnetic coupling interactions and the significant single-ion effects of octahedral cobalt(II) centers, the observed data has usually not been fitted. Strongly antiferromagnetic[19] and ferrimagnetic[41] cobalt(II) cubanes are known. The ferrimagnetically coupled Co_4(dipivaloylmethanyl)$_4$-$(CH_3O)_4(CH_3OH)_4$ system was modeled as a pair of interacting $S = 3$ units (two ferromagnetically coupled $S = 3/2$ centers), ignoring any single-ion effects.[39] A tetranickel(II) cubane cluster containing ligand **3** is ferromagnetically coupled,[21] while a mixed-valent manganese(II/III) cubane with the same ligand exhibits single-molecule magnet properties.[42]

Conclusion

Although hydrogen-bonded helicates may be reliably produced from ligand **1** and certain cobalt(II) salts under a specific set of reaction conditions, we have identified a wide range of factors which disrupt this self-assembly process including the presence of added base, the nature of the counteranion, and the structure of the ligand. As noted by Williams et al., it is "often difficult if not impossible to answer the question why one polynuclear complex is obtained rather than another",[43] and we have certainly encountered a similar quandary in the course of this work. The susceptibility of self-assembly processes involving structurally simple pyridine-alcohol ligands to be diverted from the formation of hydrogen-bonded helicates may perhaps be attributed to the lack of information stored in the ligands. This means that for any given reaction, several minima on the potential hypersurface may be close in energy and their relative energies easily perturbed by subtle changes in the reaction conditions. Solubility factors may also be important: there is an inherent bias in this work toward complexes of low solubility as X-ray crystallography was used as the primary means of characterizing the reaction products. Unfortunately, the low solubility of the majority of these products precluded a thorough investigation of their solution chemistry.

Experimental Section

General. IR spectra were recorded as Nujol mulls on a Shimadzu FTIR-8000 instrument. ES-MS spectra were recorded on an Applied Biosystems Mariner spectrometer at a concentration in the range of $10^{-4}-10^{-6}$ M. Nozzle potentials and temperatures (50−70 °C) were kept low to minimize fragmentation. Microanalyses were performed by the Toray Research Center, Eigiyoo, Tokyo. Reagents were purchased from Wako, TCI, or Aldrich and were used as received. $[Co_2(\mathbf{1})_2(\mathbf{1}-H)_2Cl_2]$ was synthesized as previously described.[1,2]

X-ray Crystallography. The X-ray crystallographic results are summarized in Table 2. Data were collected using a Bruker APEX system with Mo K_α radiation and were corrected for Lorentzian, polarization, and absorption (except for $[Co_4(\mathbf{2}-H)_6Cl_2]$ where no absorption correction was necessary) factors. Structures were solved by direct methods and refined against $|F|^2$

(40) (a) Soler, M.; Wernsdorfer, W.; Sun, Z.; Ruiz, D.; Huffman, J. C.; Hendrickson, D. N.; Christou, G. *Polyhedron* **2003**, *22*, 1783−8. (b) Aubin, S. M. J.; Sun, Z.; Eppley, H. J.; Rumberger, E. M.; Guzei, I. A.; Folting, K.; Gantzel, P. K.; Rheingold, A. L.; Christou, G.; Hendrickson, D. N. *Polyhedron* **2001**, *20*, 1139−45. (c) Aubin, S. M. J.; Sun, Z.; Eppley, H. J.; Rumberger, E. M.; Guzei, I. A.; Folting, K.; Gantzel, P. K.; Rheingold, A. L.; Christou, G.; Hendrickson, D. N. *Inorg. Chem.* **2001**, *40*, 2127−46.

(41) Tsohos, A.; Dionyssopoulou, S.; Raptopoulou, C. P.; Terzis, A.; Bakalbassis, E. G.; Perlepes, S. P. *Angew. Chem., Int. Ed. Engl.* **1999**, *38*, 983−5.

(42) Yoo, J.; Yamaguchi, A.; Nakano, M.; Krzystek, J.; Streib, W. E.; Brunel, L.-C.; Ishimoto, H.; Christou, G.; Hendrickson, D. N. *Inorg. Chem.* **2001**, *40*, 4604−16.

(43) Isele, K.; Franz, P.; Ambrus, C.; Bernardinelli, G.; Decurtins, S.; Williams, A. F. *Inorg. Chem.* **2005**, *44*, 3896−906.

Table 2. X-ray Crystallographic Data Collection and Refinement Parameters

	$[Co_4(\mathbf{1}-H)_4Cl_4(H_2O)_3MeOH)]\cdot MeOH\cdot 0.5H_2O$[a]	$[Co_4(\mathbf{1}-H)_6(NO_3)_2]$	$[Co_3(\mathbf{1}-H)_3Cl_3(dmso)]\cdot H_2O$[b]	$[Co(\mathbf{1})_2SO_4]_\infty$	$[Co_4(\mathbf{2}-H)_6Cl_2]\cdot 2CH_2Cl_2$
formula	$C_{30}H_{47}Cl_4Co_4N_4O_{9.50}$	$C_{21}H_{24}Co_2N_4O_6$	$C_{23}H_{32}Cl_3Co_3N_3O_5S$	$C_{14}H_{18}CoN_2O_6S$	$C_{31}H_{26}Cl_3Co_2N_3O_3$
fw	923.25	546.30	745.72	401.3	712.74
temp (K)	200(2)	110(2)	110(2)	110(2)	100(2)
crystal system	monoclinic	triclinic	triclinic	triclinic	triclinic
space group	$C2/c$	$P\bar{1}$	$P\bar{1}$	$P\bar{1}$	$P\bar{1}$
a (Å)	14.966(2)	9.399(2)	11.462(1)	8.4393(6)	10.927(3)
b (Å)	17.357(2)	11.475(2)	11.795(1)	8.5797(6)	11.867(3)
c (Å)	31.227(4)	11.919(2)	11.927(1)	12.0728(9)	13.562(3)
α (deg)	90	110.938(2)	80.805(2)	81.842(1)	102.892(4)
β (deg)	102.650(2)	91.528(3)	67.301(2)	84.060(1)	110.558(4)
γ (deg)	90	107.942(3)	86.474(2)	64.008(1)	108.818(4)
V (Å^3)	7915(2)	1128.6(3)	1468.3(2)	776.9(1)	1442(1)
Z	8	2	2	2	2
μ (mm^{-1})	1.972	1.515	2.057	1.274	1.468
reflns measured/unique	24521/9087	6824/4813	9202/6415	4752/3363	8501/6315
reflns obsd ($I > 2\sigma I$)	5374	4190	4278	3215	2267
R1 ($I > 2\sigma I$)	0.071	0.067	0.053	0.030	0.054
wR2 (all data)	0.201	0.212	0.113	0.080	0.093

[a] The H atoms of the free and coordinated H_2O molecules and the alcohol H atom of the MeOH ligand could not be located. [b] The H_2O molecule was found to be disordered over two positions, and its H atoms could not be located.

using anisotropic thermal displacement parameters for all non-hydrogen atoms. Hydrogen atoms attached to carbon atoms were placed in calculated positions and refined with a riding model. All other hydrogen atoms were located on the electron density difference maps.

Magnetic Measurements. Magnetic susceptibility data were collected using a Quantum Design SQUID MPMS-XL7 magnetometer working from 300 to 1.8 K at a field strength of 1 T, unless otherwise specified. Polycrystalline samples were packed into gelatin capsules, which were mounted in low-background diamagnetic plastic straws. The data were corrected for the diamagnetism of the constituent atoms using Pascal constants.[25]

Synthetic Procedures. $[Co_4(\mathbf{1}-H)_4Cl_4(H_2O)_3(CH_3OH)]$. Ligand **1** (75.4 mg, 0.61 mmol) was dissolved in MeOH (0.3 mL), and a solution of $CoCl_2\cdot 6H_2O$ (72.8 mg, 0.31 mmol) in MeOH (1 mL) and an aqueous NaOH solution (1M, 310 μL, 0.31 mmol) were added. The crimson solution was refrigerated to give a red-pink crystalline precipitate which was filtered off, washed with cold MeOH and Et_2O, and air-dried. Yield: 62 mg (86% based on $CoCl_2\cdot 6H_2O$). Anal. Calcd (Found) for $[Co_4(\mathbf{1}-H)_4Cl_4(H_2O)_3(CH_3OH)]\cdot 3(H_2O)\cdot(CH_3OH)$ ($C_{30}H_{52}Cl_4Co_4N_4O_{12}$): C, 34.70 (34.5); H, 5.05 (4.8); N, 5.40 (5.2). IR (cm^{-1}): 3200 (br, m), 1607 (m), 1576 (m), 1362 (m), 1163 (m), 1063 (s), 1015 (m), 785 (m), 648 (m).

$[Co_4(\mathbf{1}-H)_6(NO_3)_2]$. Ligand **1** (78.2 mg, 0.64 mmol) was dissolved in MeOH (1 mL), and a solution of $Co(NO_3)_2\cdot 6H_2O$ (123 mg, 0.42 mmol) and NEt_3 (89 μL, 0.64 mmol) in MeOH (1 mL) was added. Dark red crystals began forming almost immediately. The reaction mixture was allowed to stand at room temperature for 1 h before the crystals were filtered off and washed with MeOH and Et_2O. Yield: 102 mg (59%). Anal. Calcd (Found) for $C_{42}H_{48}Co_4N_8O_{12}$: C, 46.17 (45.5); H, 4.43 (4.6); N, 10.26 (10.2). IR (cm^{-1}): 2922 (br s), 1603 (m), 1574 (m), 1354 (m), 1296 (br m), 1215 (m), 1163 (m), 1113 (m), 1082 (br, m), 789 (s), 737 (w), 723 (w), 660 (m).

$[Co_3(\mathbf{1}-H)_3Cl_3(dmso)]$. Ligand **1** (33.1 mg, 0.27 mmol), NEt_3 (27.0 mg, 0.27 mmol), and $CoCl_2\cdot 6H_2O$ (64.0 mg, 0.27 mmol) were combined in dmso (1 mL) to give a deep blue solution. MeOH (1 mL) was layered on top of this solution, and deep violet prismatic crystals formed after the mixture stood at room temperature for several hours. The crystals were filtered off, washed with MeOH and Et_2O, and air-dried. Yield: 59.6 mg (91%). Anal. Calcd (Found) for $C_{23}H_{30}Cl_3Co_3N_3O_4S$: C, 37.96 (38.1); H, 4.16 (4.3); N, 5.77 (5.5). IR (cm^{-1}): 1603 (m), 1576 (m), 1362 (m), 1076 (s), 999 (m), 920 (s), 783 (s), 665 (s).

$[Co(\mathbf{1})_2(SO_4)]_\infty$. Ligand **1** (99.8 mg, 0.81 mmol) was dissolved in MeOH (3 mL), and a solution of $CoSO_4\cdot 7H_2O$ (115 mg, 0.41 mmol) in MeOH (0.5 mL) was added. The solution was refrigerated, and pink block-shaped crystals formed. Yield: 85 mg (52%). Anal. Calcd (Found) for $C_{14}H_{18}CoN_2O_6S$: C, 41.90 (41.6); H, 4.52 (4.6); N, 6.98 (6.8). IR (cm^{-1}): 2602 (br, m), 1605 (s), 1580 (m), 1364 (m), 1255 (m), 1074 (vs), 982 (m), 793 (s), 635 9m), 604 (m).

$[Co_4(\mathbf{2}-H)_6Cl_2]$. Ligand **2** (134 mg, 0.84 mmol) was dissolved in CH_2Cl_2 (2 mL), and a mixture of $CoCl_2\cdot 6H_2O$ (33.5 mg, 0.14 mmol) and $Co(OAc)_2\cdot 4H_2O$ (105 mg, 0.42 mmol) in MeOH (1 mL) was layered on top of this solution. The reaction mixture was refrigerated, and brown crystals formed which were filtered off and dried under vacuum at room temperature. Yield: 143 mg (81%). Anal. Calcd (Found) for $C_{60}H_{48}Cl_2Co_4N_6O_6$: C, 57.39 (57.5); H, 3.85 (4.0); N, 6.69 (6.5). IR (cm^{-1}): 1508 (m), 1325 (m), 1260 (m), 1101 (m), 842 (m), 827 (m), 748 (m), 738 (m). ES-MS (acetone): 747.1 ($[Co_2(\mathbf{2})(\mathbf{2}-H)_3]^+$, 25%), 535.1 ($[Co(\mathbf{2})_2(\mathbf{2}-H)]^+$, 35%), 376.1 ($[Co(\mathbf{2})(\mathbf{2}-H)]^+$, 100%).

Acknowledgment. We gratefully acknowledge the assistance of Mr. T. Sato with the X-ray crystallography. D.B.L. and J.L. thank NSERC of Canada for financial support.

Supporting Information Available: Crystallographic data in CIF format and a figure of the $[Ni_2(\mathbf{2})_3(\mathbf{2}-H)_3]$. This material is available free of charge via the Internet at http://pubs.acs.org.

IC0517218